EUROJOIN 7 GNS 5

Venezia Lido, 21 - 22 May 2009

Technical Session
Reliability of welded components and structures

ASSESSMENT OF SAFE LIFE INSPECTION INTERVALS FOR FORGED AXLES/ROTORS: THE INFLUENCE OF IN SERVICE NDT RELIABILITY (POD CURVE)

CANTINI STEFANO *- LUCCHINI RS, INNOVATION AND QUALITY DEPT., LOVERE (BG), ITALY*

PATELLI GLAUCO - LUCCHINI RS, INNOVATION AND QUALITY DEPT., LOVERE (BG), ITALY

BERETTA STEFANO - POLITECNICO DI MILANO, MECHANICAL ENGINEERING DEPT., MILANO, ITALY

CARBONI MICHELE - POLITECNICO DI MILANO, MECHANICAL ENGINEERING DEPT., MILANO, ITALY

Sommario / Summary

A new scientific approach for the assessment of safe life in service inspection intervals now takes into account both fracture mechanics parameters, in service loadings and NDT reliability. The driving application has been the increasing demand for the reliability assessment of railways components, especially for high speed trains applications. This leads to a new definition of safety factor that can be determined by a "defect tolerant" approach and by the evaluation of "safe life" inspection intervals as a function of materials characteristics, propagation models and NDT inspections. The present paper deals with the influence on inspection intervals of railways axles given by different POD curves of different NDT techniques. Initially, the POD curve of an innovative bore probe has been derived by means of dedicated experimental UT measurements and the CIVA® 8.1 software. This curve has then been exploited together with the crack propagation behaviour of the reference material in order to define inspection intervals of high speed railway axles. The results have been compared to more traditional end scan UT techniques. This approach is suitable for all kinds of rotors employed in power generation fields, aeronautics and navy fields.

1. INTRODUCTION

The early fatigue studies, performed firstly by Braithwaite and then systematically developed by Wöhler, in 19th century [1], were prompted by in service failures of railway axles.
With the development of mechanical industry, in service fatigue phenomena became a daily topic for both design and maintenance engineers.
The problem of fatigue strength estimation of components like railways axles or rotor shafts is of great importance for the transport or power generation industry, as their failures may cause serious accidents.
On the other side, the design of such components is, generally, regulated by technical recommendations which are essentially based on standard steel mechanical properties and on the definition of maximum permissible fatigue stress in a given load combination acting on the component.
Beside this classical approach, there is an increasing demand for the reliability assessment of these components, especially considering the safe life inspection intervals [2,3] and the high speed train applications, or residual life estimation for power generator shafts.
Particularly, fatigue life of railway axles can, in most cases, overcome 30 years [4] and, during this period, they are regularly inspected by means of non-destructive tests (NDT) techniques.
The inspection interval can be defined as the distance that can be safely run between two NDT controls. This interval is a function of (Fig. 1a): i) the minimum detectable crack (defect) size ($a_{50\%}$); ii) the crack propagation curve (da/dN); iii) the critical stress intensity factor (SIF) before rupture (K_{IC}).
In order to reduce the Total Life Cycle Cost of the wheel-set, an optimisation of inspection intervals of railways axles is needed. So, the three guidelines to increase inspection intervals can be:

- Upgraded materials development, aiming to higher toughness, which corresponds to an higher a_{max}, and higher resistance to crack growth, which means limited fatigue crack growth rate and a reduction of the slope of the curve in Fig. 1a;
- Fatigue crack growth (FCG) algorithms optimisation, aiming to describe crack propagation under variable loads and as a function of real component geometry, assessing a more precise description of curve in Fig. 1a;
- NDT reliability improvement, aiming to a lower crack detection threshold that leads to a reduction of $a_{50\%}$.

Since the first and the second aspects have already been previously faced by the authors [5,6], the present paper is mainly focused onto the NDT aspect of inspection intervals. A brief description about the procedure here applied in order to derive the POD ("Probability of Detection") of a defect is then given in the following paragraph.

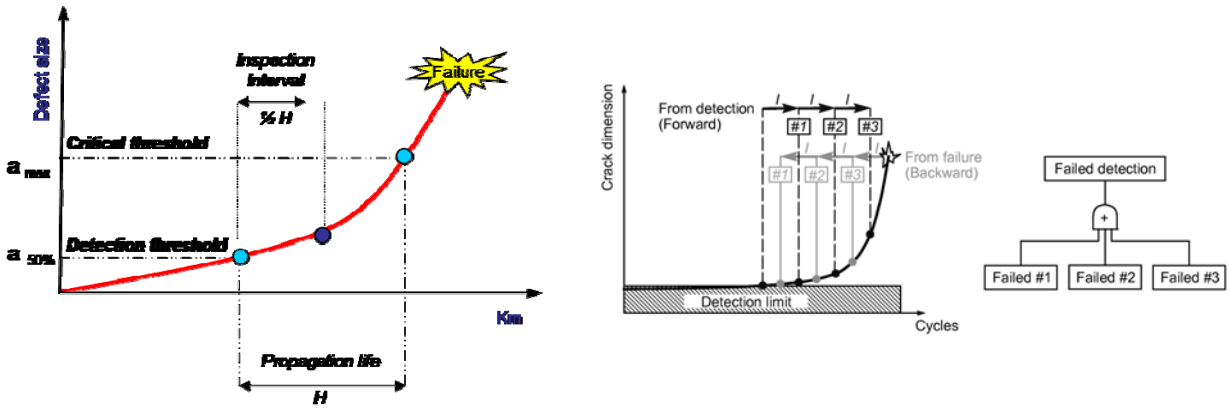

(a) **(b)**

Fig. 1: a) Inspection intervals representation;
Fig. 1: b) definition of "forward" and "backward" cumulative probability of detection.

1.1 Cumulative probability of detection of a defect

A simple definition (Fig. 1a) of inspection interval is to fix it to half the propagation life from detection of the crack to its critical size. However, since detection is characterised by a POD curve (larger is the crack, larger is the probability of detection), it is more suitable to adopt a cumulative probability of detection.

Given an inspection interval "I", the probability of detection of a defect, potentially observable in a given number of inspections "i" derived from the POD curve of the adopted NDT technique, is calculated. Fig. 1b, in which three inspections are assumed and where the concepts of "forward" and "backward" inspections are also introduced, shows this approach. It is necessary to add that because of the conservatorism introduced in the adoption of "backward" inspections [7], only this case will be considered in the following. The total POD of a defect can then be derived:

$$PC_{DET} = 1 - \left(\prod_i POND_i \right) \quad \textbf{(1)}$$

where PC_{DET} is the theoretical cumulative probability of detection and POND ("Probability of Non Detection") represents the probability to fail the detection. The drawback of this approach is that the repetition of inspections on cracks having very low POD (i.e. in the initial phases of propagation life) increases the PC_{DET} value, but introduces further influences (sizing errors, operator errors) typical of this stage.

1.2 High Speed Axles in service inspection

The derivation of inspection intervals has been carried out in the present research considering the special application of a 30NiCrMoV12 high strength quenched and tempered steel (according to UNI 6787-71 [9]) typically adopted by Lucchini RS for production of hollow axles mounted onto high speed trains.

In order to deeply investigate the influence of in service inspection reliability, the POD curve of an innovative bore probe [10] has been derived by means of dedicated experimental UT measurements and the CIVA® 8.1 software [11] and then compared to the POD curve of a traditional far end scan technique (under the hypothesis of comparing an hollow bored axle to a solid one).

These curves have then been used together with the crack propagation behaviour of 30NiCrMoV12 steel (derived elsewhere [5,6]) in order to define inspection intervals of high speed railway axles.

2. UT MEASUREMENTS ON HOLLOW AXLES

Some experimental UT measurements have been carried out onto cracked axles in order to define the POD curve of an innovative bore probe. In the following, a brief description of both the probe and the experiments is given.

2.1 Description of innovative bore probe

The BAT ("Bore Axle Testing") system, developed in order to fulfil Lucchini RS technical specifications, is shown in Fig. 2a. BAT is a multi-channel system, integrated by an innovative pressure/flow detector embedded on the probe-holder and a post processing unit, and allows the continuous inspection by up to eight probes in order to reduce the minimum detectable defect and optimise the POD for the most complex wheelset geometries.

A new conception probe holder (Fig. 2b), with common probes zero, has been manufactured in order to manage up to eight crystals in a compact solution. In the present research, four probes, all having frequency equal to 4 MHz, have been considered: 45° "forward" and "backward" and 38° "forward" and "backward". "Forward" means that the sound beam is directed as the ogive's tip, while "backward" in the opposite direction.

The mechanical part is composed by a battery motorized trolley and an electric cabinet on it: a motorized arm with six axis movements is present to centre the axles hole and to do the ultrasonic inspection.

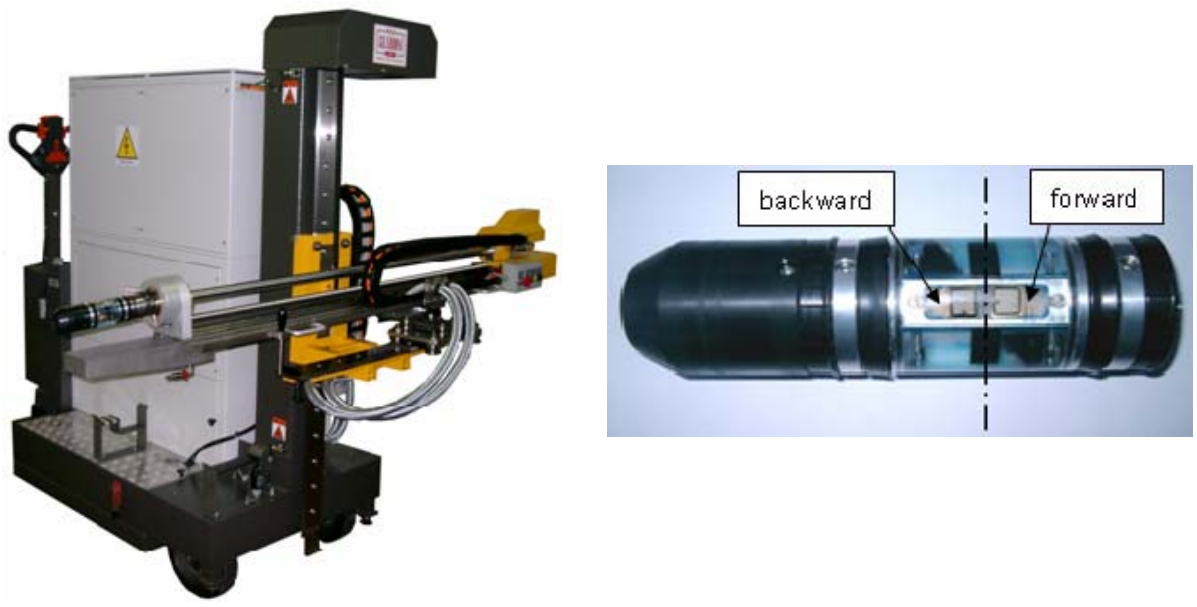

(a) **(b)**

Fig. 2: "Bore Axle Testing" system (a) and its probe-holder (b).

2.2 UT measurements

In order to get realistic back reflection echoes, an overall statistical population of 29 real fatigue cracks has been considered.

In fact, for a given probe and defined geometry, the difference between the back reflection echo of a real crack and an artificial notch of equivalent area is not negligible (an overview is shown in Fig. 3a).

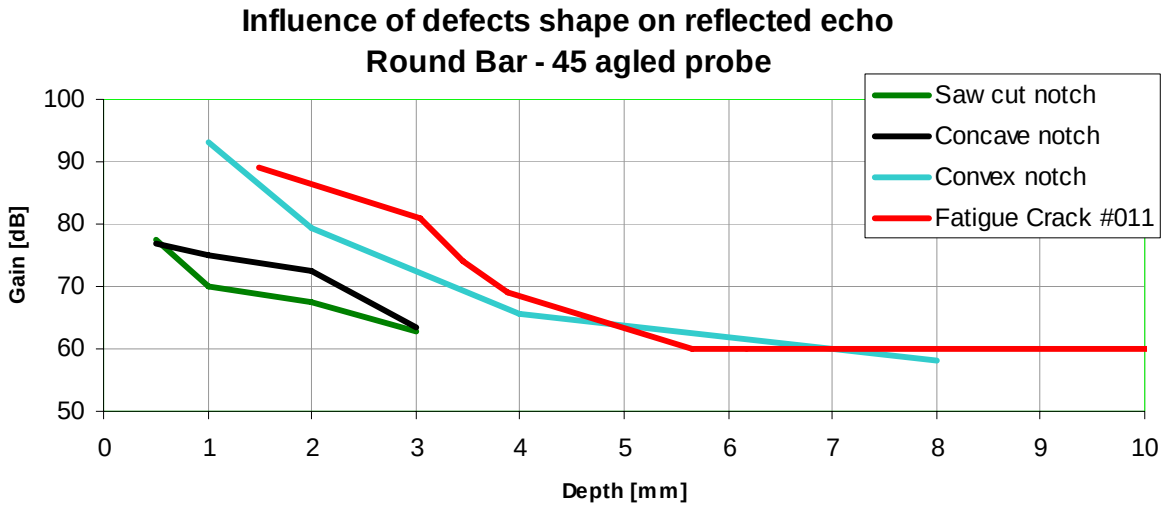

Fig. 3: Gain needed to detect different shaped defects at different depth, in round bar by means of 45° - 4MHz probe (a)

For the above reasons, the measurements were carried out on a series of axles presenting multiple fretting fatigue cracks at the press-fit seat. Actually, the here-considered geometry (Fig. 3b) of axles is referred to full-scale specimens for fatigue and crack propagation tests as described by EN13261. Fatigue tests are carried out by means of a dedicated bench (Fig. 3c) available at both Lucchini RS's and Politecnico di Milano's labs.

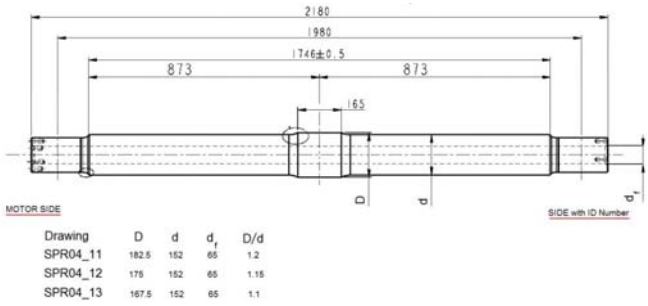

(b)

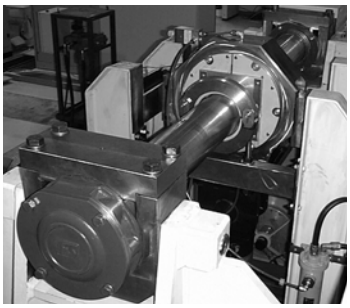

(c)

Fig. 3: Full-scale specimens for fatigue and crack propagation tests (b) and dedicated test bench (c).

Cracks were firstly evidenced by means of fluorescent MT (Fig. 4 shows an example) and quantified (in terms of depth and circumferential length) by both manual UT inspection with different angled probes and ACPD measuring system. Hollow axles were then inspected by the BAT system and the UT indications recorded in order to define the POD curve.

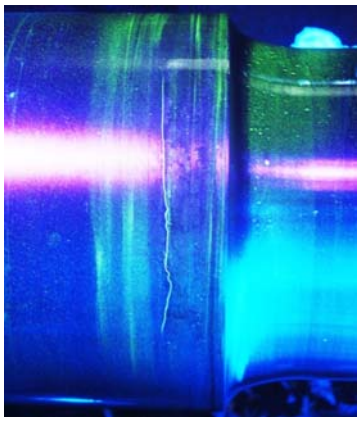

Fig. 4: Fretting crack at the press-fit seat evidenced by MT.

3. SIMULATION OF UT MEASUREMENTS ON HOLLOW AXLES

The simulation of ultrasonic NDT by a bore probe applied to bored railway axles in 30NiCrMoV12 steel has been carried out by means of CIVA® v.8.1 software [11]. Two different kind of pulse-echo analyses were carried out: the first one involving the simulation of UT measurements on the sample block used by Lucchini for determining TGS, with the aim to check the ability of the software to catch experimental results; the second one involves the simulation of UT measurements in bored axles presenting different geometries of defect positioned in two different critical zones: the T-transition and the press-fit seat.

In all the simulations, the modelled material represents the 30NiCrMoV12 steel and it is important to add that dedicated experiments have been carried out about the transparency of this steel finding that material attenuation of sound waves is negligible at both 2 and 4 MHz. The value for velocities has been set to 5920 m/s for longitudinal waves and 3230 m/s for transversal waves.

3.1 Simulation of sample block experimental UT measurements

The schematic of the sample block [12] is shown in Fig. 5. Every section of the sample block has been modelled using CIVA®. Figg. 6a and 6b show the example of the section having diameter equal to 120 mm (the bore has diameter equal to 65 mm in every section). From this figures it is also interesting to note the prospective sound path represented by a simple ray-tracing technique.

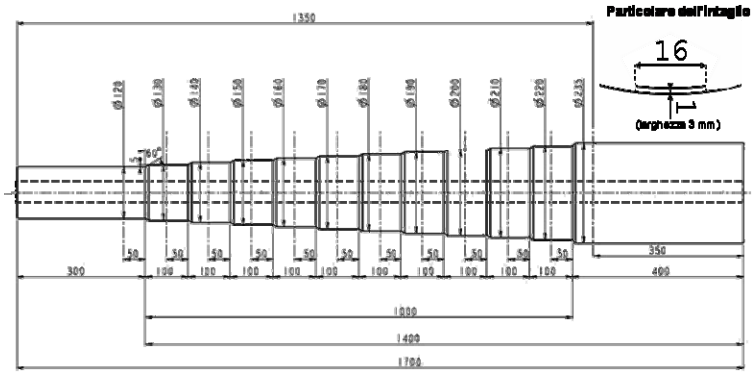

Fig. 5: Sample block for determining DAC (or TGS) curve [15].

Particular attention has been paid in modelling the artificial defects (Fig. 6c) and the probe (Fig. 6d).

Regarding the probe, both the dimensions of the crystal and of the wedge in plexiglas (V_L=2680 m/s and V_T=1320 m/s) have been modelled exactly as in the real bore probe and following the transducer data sheet provided by the producer. The same can be said for the transmitted signal shape reconstructed in CIVA® starting from its experimentally determined frequency content. Finally, simulations have been carried out for both the 45° and the 38° probes (both 4 MHz).

The tests have been simulated letting the probe move longitudinally along the sample block from 5 mm before till 5 mm after the defect with a step of advancement equal to 0.5 mm. The coupling medium has been modelled to be oil as in the real bore probe. Since CIVA® works considering mainly signal amplitudes, the dB values from echoes have been here computed considering, as a reference value, the amplitude of the transmitted signal (always the same during every analysis).

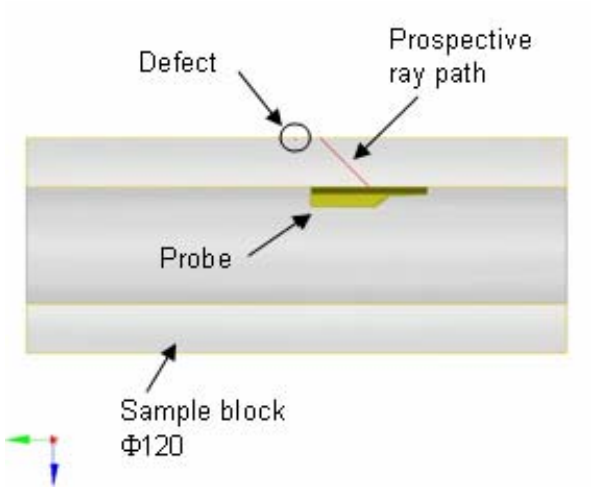

(a)

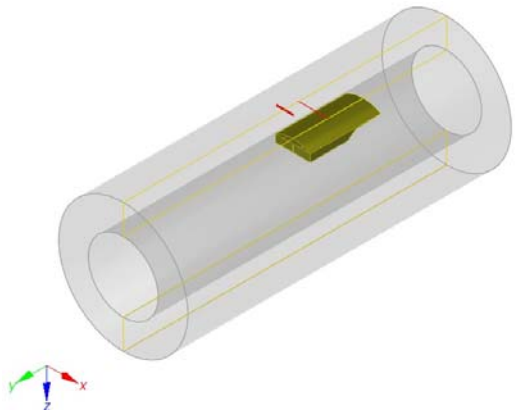

(b)

Fig. 6: CIVA® model of the sample block (a) and (b)

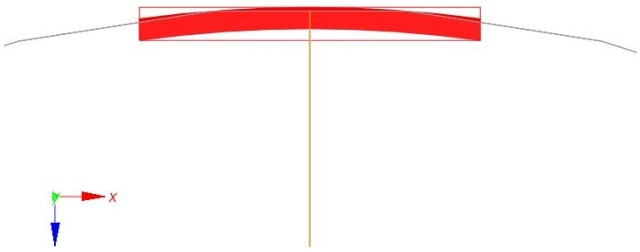

(c)

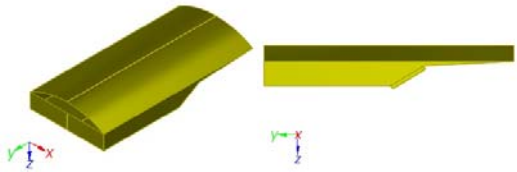

(d)

Fig. 6: CIVA® defect (c) and probe (d).

Fig. 7a shows the B-scan obtained from the simulation for the case of diameter equal to 120 mm, while Fig. 7b the A-scan extracted from the B-scan in correspondence of the highest echo. Repeating the procedure for all the sections of the sample block and for both the 45° and 38° probes, the comparison between simulated and experimental TGS curves is possible (Fig. 8). The results seem to be encouraging since the predicted TGS curves are very near to the experimental ones.

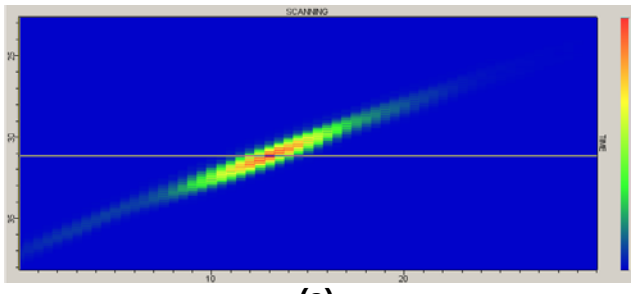

(a)

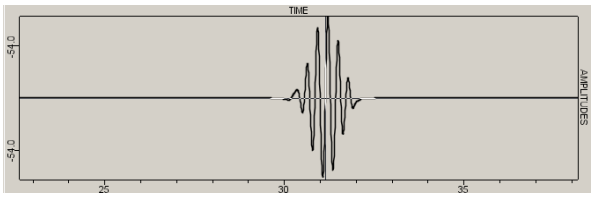

(b)

Fig. 7: Results obtained in the case of diameter equal to 120 mm: a) B-scan;
Fig. 7: b) A-scan corresponding to the highest echo.

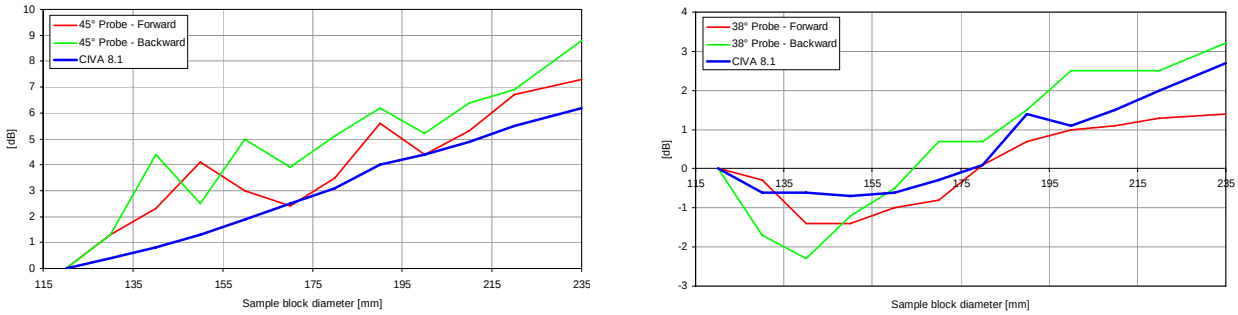

(a) **(b)**

Fig. 8: TGS curves for 45° (a) and 38° (b) probes.

3.2 Simulation of defects in axles and POD curve determination

In order to reduce the time of calculation, only a part of the axle has been modelled (Fig.9): the considered part includes the body, the T-transition and the press-fit seat. Two different kind of defects have been considered: convex defects (as a fatigue crack, typically on the body at transitions) and concave defects (as a fretting crack, typically on the press-fit seat). The considered defects depths “d” were 0.5; 1; 2; 3; 5; 10; 15 and 20 mm. In particular (Fig. 9), at the press-fit the defects were put at 10 mm from the seat edge and at the T-transition they were put at the notch root. All the other parameters for the simulations have been taken identical to what described in the previous paragraph. The simulations were carried out observing the defects with both forward and backward probes.

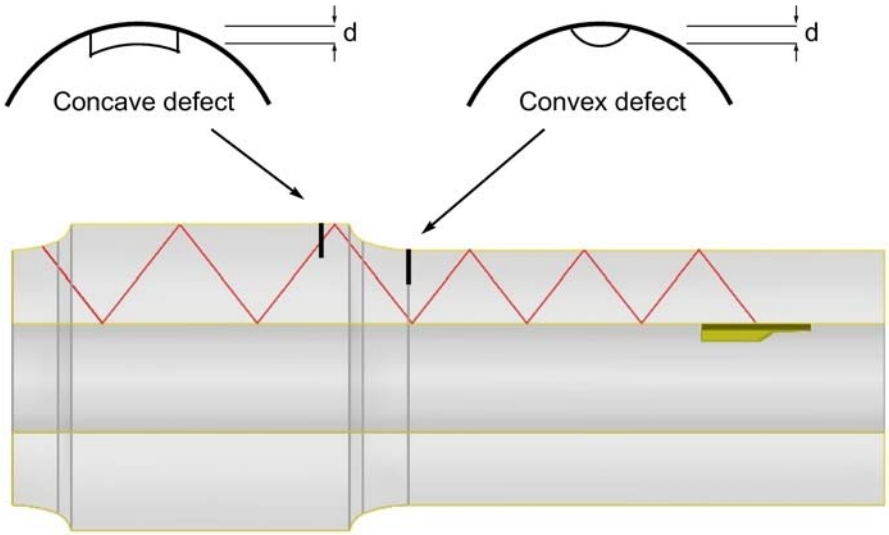

Fig. 9: Simulation of defects in axles.

For the present research, the most interesting zone of the axle is the T-transition but, unfortunately, no axles, cracked in this region, were available for experimental inspection. So, with the aim to transpose experimental results from the press-fit seat to the T-transition, the relevant result obtained from numerical simulations has been the difference in signal amplitude between the concave defect at the press-fit seat and the convex defect at the T-transition with the hypothesis that the two defects present the same depth. The convex defect at T-transition in general resulted to be less sensible than the other one for a quantity equal to 1.5 dB for a relatively large crack (a>5 mm). This value includes two different effects: the different time of flight (T-transition is nearer to the probe) and the different reflecting area (the convex defect has smaller area than the concave one having the same depth).

The obtained result permitted then to derive the POD curves for the BAT system at both the press-fit seat and the T-transition by opportunely changing (Fig. 10a) the reference dB value into the usual analysis for determining POD curves [13]. Fig. 10b shows the obtained theoretical curves compared with the one relative to the traditional Far End Scan [14] and the suitable curve, for inspection interval determination, characterised by the truncation of crack depth values smaller than 1 mm (i.e. the depth of calibration slots).

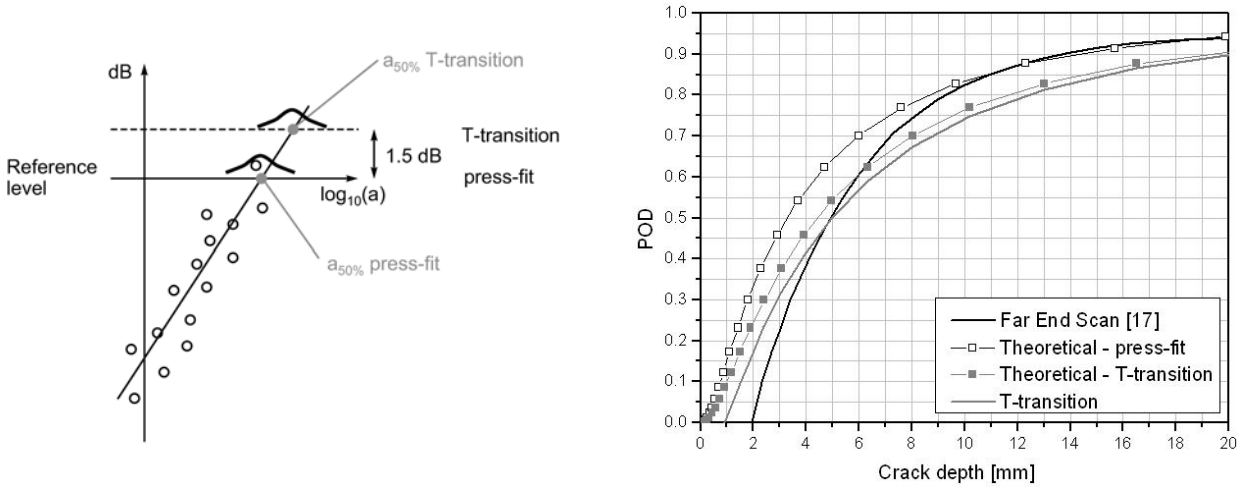

(a) **(b)**

Fig. 10: Determination of BAT POD curve: a) schematic of the procedure;
Fig. 10: Determination of BAT POD curve: b) POD curves resulting from the analyses.

4. DETERMINATION OF INSPECTION INTERVALS

In order to determine inspection intervals, the crack behaviour of the considered steel must be introduced. In the present paragraph, the results previously obtained by the authors [8,10] are briefly summarised before proceeding to the calculation of inspection intervals.

4.1 Analysis of crack growth

30NiCrMoV12 steel basic mechanical properties are : tensile strength R_m = 1050 MPa, yield strength $R_{p0.2}$ = 995 MPa, reduction of area Z= 67%, fracture toughness at 20°C K_{IC} = 120 MPa$\sqrt{m}$, impact test at room temperature (U notch) K_{CU}= 70 J, cyclic yield strength $R_{p0.2cyc}$ = 730 MPa, Vickers hardness 330 HV and fatigue limit at R= -1 σ_{wo} = 525 MPa.

Service loads of railway axles are the result of vertical and lateral forces (EN13103 and EN13104 acting on them due to the typical operations: it is worth noting that the maximum stresses can be found in proximity of the wheel press-fit. On the basis of these considerations, fatigue crack growth at the T-transition has been analyzed considering a load spectrum (Fig. 11) experimentally derived [5] on a Pendolino train and corresponding to 10^7 km of Italian railway lines.

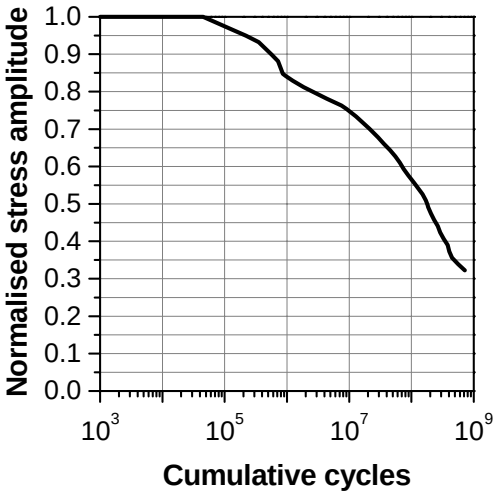

Fig. 11: Normalized cumulative load spectrum corresponding to 10^7 km onto Italian railway lines [5].

In literature, different analytical algorithms for life prediction of cracked bodies are available: in the present study, NASGRO v. 3.0.21 [15] has been considered. Such a choice is due to the fact that this software is one of the reference points for analyses under variable amplitude loads. Particularly, NASGRO keeps into account for the different effects acting on crack growth rate in metallic materials (stress ratio, load interaction effects) by simulating the "plasticity induced crack closure" phenomenon [16]. This phenomenon is the consequence of crack tip plasticity (in terms of residual stresses and plastic wakes) and its effect is that the opening (and propagation) of the crack occurs for applied stresses bigger than the P_{op} value.

The analytical model is based on the so-called "NASGRO Equations" [15]. The first one is able to describe crack growth rate ("da/dN") as a function of the stress intensity factor ("ΔK") for all the three propagation regimes (threshold, Paris and critical), while the second one describes the threshold ("ΔK_{th}") variation as a function of the stress ratio ("R"). Calibration of the empirical parameters present in these equations is carried out by means of dedicated Fracture Mechanics experiments: in the case of the 30NiCrMoV12 steel, the calibration has already been achieved by the authors in previous researches [6,8].

The considered load spectrum have been applied in terms of constant amplitude block loads arranged adopting a Gassner sequence [13] characterized by R = -1, i.e. the typical operational condition for railway axles. Moreover, block loads were applied in terms of plane bending since NASGRO is not able to consider rotating bending conditions.

The axle was modeled in terms of a smooth circular tube having external diameter equal to 152 mm and internal diameter equal to 65 mm in order to analyze the fracture behaviour of the body. Stress concentration at the T-transition was considered multiplying the stress amplitudes of the spectrum for a stress concentration factor K_t=1.22 [17]. A penny shaped crack having a depth equal to 2 mm (a value certainly conservative for impacts due to the ballast [18]) was considered as initial flaw, while 43 mm was adopted as the limiting crack depth value at failure. Results are reported in Fig. 12.

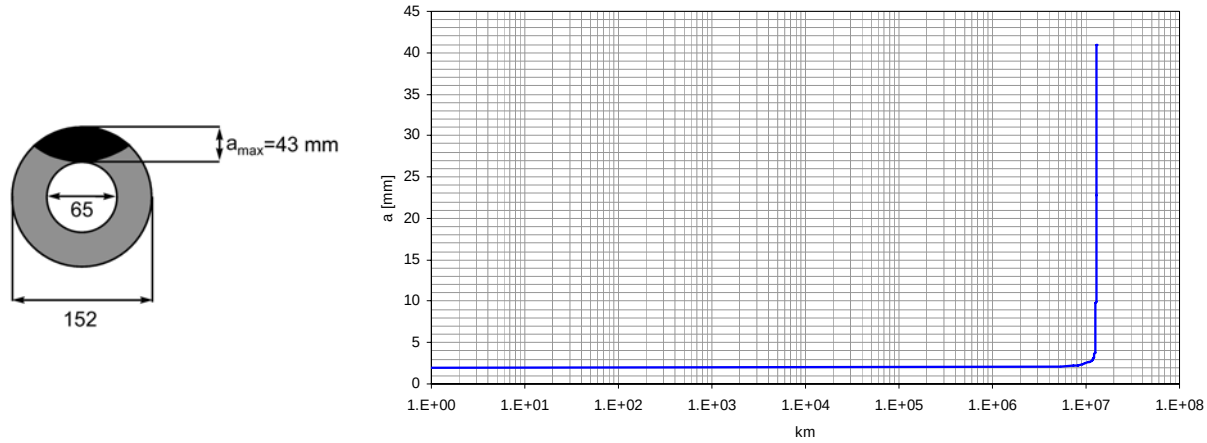

Fig. 12: Life estimate obtained from the considered load spectrum.

4.2 Inspection intervals

The analysis of the POD of cracks, based on Eq. (1), has been carried out in terms of variation of the inspection interval expressed in kilometres. Fig. 13a shows the obtained PC_{DET} results considering the BAT POD curve and the traditional Far End Scan POD curve.
In general, it seems that BAT yields better performances in respect to traditional Far End Scan. Considering the length of the inspection interval adopted for the axles of Pendolino train (typically equal to 200.000 km), Fig. 13b shows that the PC_{DET} value obtained using BAT is equal to 1, while the value obtained from Far End Scan is a little bit lower. Moreover, fixed any PC_{DET} value, BAT always yields longer inspection intervals: for example, considering a PC_{DET} value equal to 0.99, the length of the inspection interval using BAT should be set equal to 550.000 km, while using traditional Far End Scan equal to 210.000 km. This can seem strange since BAT POD curve is higher than the Far End Scan one only for small crack depths (less than about 5 mm), but it should also be noted from Fig. 12 that this crack depth is reached just before the final failure.
Finally, from the operating point of view, it must be remarked that BAT technique makes possible to inspect the whole axle with constant angles between probes and inspected volume, while End Scan technique does not permits the inspection of different parts of the axle at the same time with constant sensibility.

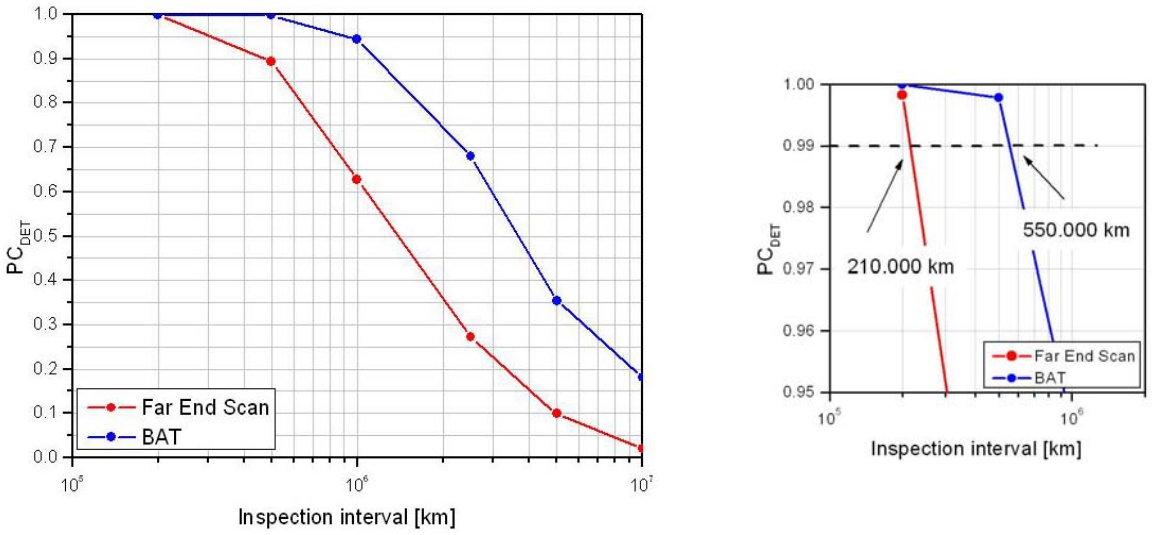

(a) (b)

Fig. 13: Cumulative probability of detection vs. inspection interval.

5. CONCLUSIONS

A definition of inspection intervals for axles/rotor shafts has been proposed with particular focus on railways axles; this involves also a “defect tolerant” approach and a probabilistic analysis of in service NDT inspections reliability.
For railways axles, POD curves have been assessed on press fit area and then transposed to T-transition notch area by means of validated and dedicated software.
A first comparison between a new UT device and the standard far end scan technique has been proposed.
Crack propagation life has been simulated by a validated model tuned on 30NiCrMoV12 steel grade which is widely employed for high speed trains but also for aeronautics and power generation fields.
The knowledge of both POD, in service real loads and crack propagation properties for a given application, is a powerful tool to:

- design inspection intervals given in service loads and NDT technique
- design NDT technique improvements, by means of a dedicated fine tuned software, in order to extend in service inspection intervals

In a nutshell, the possibilities to reduce TLCC of safety critical components like railways wheelsets by the aid of fully customized inspection procedures is now more close to reality.

6. IN PROGRESS

Nowadays the working Group leaded by Lucchini RS in cooperation with Politecnico di Milano is focusing the attention on the following:

- Increase Statistical population of fatigue cracks by means of dedicated experiment aiming to propagate fatigue cracks in T-transition notches.
- Preliminarily validate in service NDT techniques (i.e. phased array) by means of both numerical model and experimental measurements on existing fatigue cracks base
- Collecting in service real spectra by means of instrumented wheelsets

6. REFERENCES

[1] TIMOSHENKO, S.P. 1983, Dover Publications Inc., New York.
[2] SMITH, R.A. *et al.:* In: *Proc. 13th Int. Wheelset Congress*. 2001, Roma, Italy.
[3] ZERBST, U. *et al.: Eng. Fract. Mech.* 72, 2003, 209.
[4] STONE, D.H. *et al.: J. Rail and Rapid Transit* 218, 2004, 357.
[5] CANTINI, S. *et al.:* In: *Proc. 14th Int. Wheelset Congress*. 2004, Orlando, USA
[6] BERETTA, S. *et al.:* In: *Fatigue and Fracture Mechanics: 34th Volume, ASTM STP 1461*. 2004, S. R. Daniewicz, J. C. Newman and K.-H. Schwalbe, Eds., ASTM International, West Conshohocken, PA.
[7] BERETTA, S. *et al.: J. Rail and Rapid Transit* 218, 2004, 317.
[8] BERETTA, S. *et al.: Eng. Fract. Mech* 73, 2006, 2627.
[9] UNI 6787-71: Italian National Standardisation Bureau, 1971.
[10] GILARDONI C. *et al.:* In: *Proc. 15th Int. Wheelset Congress*. 2007, Prague, Czech Republic.
[11] CEA: *CIVA 8 User Manual*, Website: http://www-civa.cea.fr.
[12] G. PATELLI *et al.: Technical Instruction QUA T.I. 065 Rev.5*. 2007, Lucchini Sidermeccanica S.p.A., Lovere (BG), Italy.
[13] GEORGIU, G.A.: *Research Report 454*. HSE Books, Health and Safety, Executive, UK.
[14] BENYON, J.A. *et al.:* In: *Proc. 13th Int. Wheelset Congress*. 2001, Roma, Italy.
[15] NASA: *NASGRO User Manual*, Website: www.nasgro.swri.org.
[16] ELBER, W.: In: *ASTM STP* 486, 1971, 230.
[17] CARBONI, M. *et al.:* Accepted for publication on *J. Rail and Rapid Transit.*
[18] GRAVIER, N. *et al.: Revue générale des chemins de fer* 3, 1999, 33.